ELSEVIER

Journal of Power Sources 110 (2002) 186–200

JOURNAL OF POWER SOURCES

www.elsevier.com/locate/jpowsour

Thermodynamic and transport properties of gases for use in solid oxide fuel cell modelling

B. Todd*, J.B. Young

Hopkinson Laboratory, Cambridge University Engineering Department, Trumpington Street, Cambridge CB2 1PZ, UK

Received 18 October 2001; received in revised form 16 April 2002; accepted 22 April 2002

Abstract

Data are provided and estimation methods presented for the calculation of specific heat capacities, viscosities, thermal conductivities and diffusion coefficients for both pure components and mixtures of C_3H_8, C_2H_6, CH_4, H_2O, CO_2, CO, H_2, N_2, O_2 and Ar over the temperature range 273–1473 K at ambient pressure. Pure component data is assembled from various data compilations supplemented by validated estimation techniques. Fourteen estimation methods for mixture properties have been compared with each other and with over 1400 experimental data points to facilitate the choice of methods best suited to this application. A statistical analysis of the data (including expected accuracy) is presented and recommendations are made for practical use. © 2002 Elsevier Science B.V. All rights reserved.

Keywords: SOFC; SOFC modelling; Viscosity; Thermal conductivity; Diffusion; Gas mixture properties

1. Introduction

Solid oxide fuel cell (SOFC) development is entering the optimisation phase; viability has been well demonstrated but profitability has not. The key to profitability lies in integrated plant optimisation. With 'balance of plant' likely to account for a significant part of the total system cost and be responsible for most unscheduled outages [1], it is not sufficient to optimise the fuel cell stack and then construct the plant around it. Achieving a high *net* efficiency and a low *net* cost requires detailed understanding of the thermal and flow processes both within and without the stack in order to maximise output and reduce losses.

In order to meet this challenge, SOFC modelling is becoming more sophisticated and an increasing number of publications deal with stack models involving detailed descriptions of the flow, thermal, chemical and electrochemical processes. The accuracy of these models is limited, however, by the reliability of the available data for the thermodynamic and transport properties, which determine the heat and mass transfer rates and hence the limits on stack performance [2].

This paper describes a study to evaluate the accuracy and reliability of the many semi-theoretical and empirical methods available for predicting the properties of SOFC gas mixtures. Two specific problems have emerged from the study. The first involves the extrapolation of low temperature experimental data to the high temperatures (1150–1300 K) encountered in SOFC operation. The second concerns the evaluation of the transport properties of multi-component gas mixtures from pure component data. In the absence of experimental measurements, these problems are difficult to overcome. However, by using a graphical and statistical assessment of the available data, and by comparing the various extrapolation techniques, it has been possible to establish property estimation methods which should prove reliably accurate for most SOFC calculations.

2. The nature of the gases under consideration

The following gases are important in SOFC technology: C_3H_8, C_2H_6, CH_4, H_2O, CO_2, CO, H_2, N_2, O_2 and Ar. Unfortunately, the familiarity of these gases obscures the fact that they are sometimes very different in structure and physical behaviour. The two factors of particular significance are the *molecular orientation* and the *molar mass*.

Difficulties related to molecular orientation are indicated by a high dipole moment (greater than 1.0 debye, say) and also by the presence of hydrogen bonding. Simple estimation techniques are usually not applicable to polar gases and even complex methods often give unreliable results. Of the gases considered here, H_2O is highly polar with a dipole moment of 1.8 debye, CO is slightly polar (0.1 debye), and

* Corresponding author. Fax: +44-1223-332-662.
E-mail address: bt206@eng.cam.ac.uk (B. Todd).

0378-7753/02/$ – see front matter © 2002 Elsevier Science B.V. All rights reserved.
PII: S0378-7753(02)00277-X

all the other species are non-polar. The properties of H_2 are strongly affected by quantum effects.

In mixtures, the presence of gases with either very different, or very similar, molar masses sometimes result in irregular characteristics which are difficult to predict. CO_2 and C_3H_8 have almost the same, very high, molar mass of 44 kg/kmol, while H_2 (the most important fuel-side component) has a particularly low molar mass of 2 kg/kmol.

3. The origin of the estimation methods

3.1. Corresponding states

The 'law of corresponding states' was proposed by van der Waals in 1873 and expresses the generalisation that equilibrium thermodynamic properties which depend on intermolecular forces are related to the properties at the critical point in a universal way. Hence, if a property is known for one substance, its value for another may be estimated by scaling with respect to the critical properties. For simple molecules, a two-parameter model (as suggested by van der Waals) may give acceptable results but for more complex (non-polar) fluids, a third parameter is often introduced to improve accuracy. Unfortunately, corresponding states methods do not work well for gases, such as H_2 and H_2O in which molecular orientation is important.

3.2. Kinetic theory of the transport properties

Elementary kinetic theory assumes gases to consist of rigid spheres of specified mass and diameter. In the presence of bulk velocity, temperature and concentration gradients, the collisions of these spheres are responsible for the transfer of momentum (viscosity), energy (thermal conductivity) and molecular mass (diffusion). The simplest estimation techniques for the transport coefficients are based on so-called 'mean free path' theories. However, although the resulting expressions provide physical insight and indicate trends, they are insufficiently accurate for detailed SOFC calculations.

For rigorous evaluation of the transport properties, it is necessary to solve the Boltzmann equation using the Chapman–Enskog method [3]. In reality, molecules do not behave as hard spheres but attract or repel each other with intermolecular forces which vary with the separation distance between molecules and their orientation. Chapman–Enskog theory accounts for these forces by specifying a separation dependent potential energy function. Four main assumptions are involved in the theory: (i) the gas is sufficiently dilute that only binary collisions occur; (ii) molecular motion during collisions can be described by classical mechanics; (iii) only elastic collisions occur; (iv) the intermolecular potential function is spherically symmetric. The theory is thus strictly applicable only to low pressure, high temperature, non-polar gases. However, there being no tractable alternative models, it is invariably adapted for use with polar gases.

The Chapman–Enskog expressions for the transport properties have forms similar to those obtained from the 'mean free path' theories but include a 'collision integral' which must be calculated from the assumed potential energy function. The choice of this function is critical to the accuracy of the technique but again compromise is accepted in return for tractability. The potential function often used (despite its tenuous theoretical grounding for many species) is the two-parameter Lennard–Jones 12-6 potential. This can give good results for the coefficients of viscosity and diffusion but problems arise when calculating the thermal conductivity of polyatomic gases (because of the difficulty of modelling correctly the transfer of molecular internal energy).

3.3. Formulation of the estimation methods

The most successful estimation techniques use kinetic theory and/or corresponding states theory in conjunction with empirical data to formulate 'corrections' to a basic theoretical model. The rationale for this approach is that, although correlations can be made purely from empirical data, the use of a theoretical basis increases the chances of a technique remaining valid outside the data range used in its construction. Generality is clearly of great benefit but is difficult to achieve as different species highlight different weaknesses in a chosen model. For this reason no one model can be described as universally 'best' and the recommendations made below therefore represent the 'best compromise'.

The calculation of the properties of gas mixtures requires accurate pure component data. The starting point of this study has therefore been the 'Physical and Thermodynamic Properties of Pure Chemicals: Data Compilation' (PTPPC) [4]. This appears to be the most comprehensive and best validated compilation freely available. Where necessary, the PTPPC data has been extended using various other data sets. The estimation techniques used for mixture properties can be found in 'The Properties of Liquids and Gases', 4th edition [5] and 5th edition [6]. These references also list most of the required critical properties. However, in order to make the paper self-contained, all property data, together with the recommended mixture property equations, have been assembled in the Appendix A.

4. Thermodynamic properties of pure gases and gas mixtures

4.1. Isobaric molar heat capacity

At the high temperatures associated with SOFC operation, all gas mixtures can be accurately represented as mixtures of ideal (semi-perfect) gases. This implies that the molar heat capacities (C_p and C_v) are functions of temperature but not pressure. Furthermore, $C_p - C_v = R$, where R is the universal gas constant (8.3143 kJ/kmol K).

Table 1
Isobaric molar heat capacity, coefficients valid in the range 273−1473 K

	a_0	a_1	a_2	a_3	a_4	a_5	a_6	Error (%)	C_p (1473 K)
Ar	20.786	0.0	0.0	0.0	0.0	0.0	0.0	1	20.786
C_2H_6	−0.2847	268.90	−494.31	867.78	−850.96	408.07	−75.971	1	144.35
C_3H_8	−16.527	472.86	−885.76	1434.0	−1344.2	631.90	−116.65	3	203.64
CH_4	47.964	−178.59	712.55	−1068.7	856.93	−358.75	61.321	1	88.294
H_2O	37.373	−41.205	146.01	−217.08	181.54	−79.409	14.015	1	46.831
CO_2	4.3669	204.60	−471.33	657.88	−519.9	214.58	−35.992	1	58.457
CO	30.429	−8.1781	5.2062	41.974	−66.346	37.756	−7.6538	1	35.132
H_2	21.157	56.036	−150.55	199.29	−136.15	46.903	−6.4725	1	32.146
N_2	29.027	4.8987	−38.040	105.17	−113.56	55.554	−10.350	1	34.756
O_2	34.850	−57.975	203.68	−300.37	231.72	−91.821	14.776	1	36.469

C_p (kJ/kmol K) $= \sum_{k=0}^{6} a_k \tau^k$, where $\tau = T$ (K)/1000.

The PTPPC data set is complete for the required C_p data and was used to generate sixth-order polynomial curve fits using a least-squares procedure. (As a precaution, the expressions were also validated against the JANAF Thermochemical Tables [7].) The error (i.e. the deviation from the experimental data) in the curve fitting procedure was, in all cases, less than 0.1%. Table 1 gives the coefficients of the polynomials. The 'error' specified is that given by PTPPC as the uncertainty in the experimental data and is less than 1% for all species except C_3H_8 (which exhibited uncertainties up to 3%). Values of C_p at 1473 K are included as an aid for readers wishing to check coding.

The molar heat capacity of an ideal gas mixture of n component gases is given by

$$C_p(T) = \sum_{i=1}^{n} x_i C_{pi}(T)$$

where x_i and C_{pi} are the mole fraction and molar heat capacity of the ith component.

5. Viscosity and thermal conductivity of pure gases

5.1. Dynamic viscosity

The PTPPC data set for dynamic viscosity is near to complete, lacking only high temperature data for C_3H_8, C_2H_6, CH_4 and CO. This appears to be due to the lack of primary experimental data. To rectify this situation, estimation techniques were utilised, using the available PTPPC data to select the best estimation technique for each species. According to Poling et al. [6], the estimation methods of Chung et al. or Lucas should give errors of less than 1.5% for polar and 4% for non-polar gases. However, as these values are smaller than the errors quoted in PTPPC for the uncertainty in the experimental data, it is probable that the error given by PTPPC is more representative. The extended data set was then used to generate sixth-order polynomial curve fits using a least-squares procedure and the coefficients are given in Table 2. As before, the error due to the curve fitting is less than 0.1% over the temperature range 273−1473 K. Values of dynamic viscosity at 1473 K are included as an aid for readers wishing to check coding. It should be noted that the unit of viscosity is the micro-poise (1 μP $= 10^{-7}$ kg/ms).

Fig. 1 illustrates the problems associated with polar gases. Fig. 1a is for CH_4 which is non-polar and Fig. 1b is for H_2O which is strongly polar. The excellent performance of the estimation methods for CH_4 contrast strongly with the poor performance for H_2O at high temperatures.

5.2. Thermal conductivity

Thermal conductivity presents more difficulty than viscosity because there are significantly fewer experimental data

Table 2
Dynamic viscosity, coefficients valid in the range 273–1473 K

	b_0	b_1	b_2	b_3	b_4	b_5	b_6	Error (%)	η (1473 K)
Ar	−3.0982	978.51	−922.67	912.64	−593.76	217.79	−33.919	1	721.65
C_2H_6	−17.260	454.68	−324.04	213.47	−80.053	10.693	0.8929	5	338.03
C_3H_8	−7.9185	312.59	44.453	−329.65	362.08	−175.84	32.735	3	314.94
CH_4	−9.9989	529.37	−543.82	548.11	−367.06	140.48	−22.920	5	353.61
H_2O	−6.7541	244.93	419.50	−522.38	348.12	−126.96	19.591	3	553.28
CO_2	−20.434	680.07	−432.49	244.22	−85.929	14.450	−0.4564	5	514.47
CO	−4.9137	793.65	875.90	883.75	−572.14	208.42	−32.298	5	510.04
H_2	15.553	299.78	−244.34	249.41	−167.51	62.966	−9.9892	10	270.13
N_2	1.2719	771.45	−809.20	832.47	−553.93	206.15	−32.430	3	533.02
O_2	−1.6918	889.75	−892.79	905.98	−598.36	221.64	−34.754	5	632.36

$\eta(\mu\text{P}) = \sum_{k=0}^{6} b_k \tau^k$, where $\tau = T$ (K)/1000.

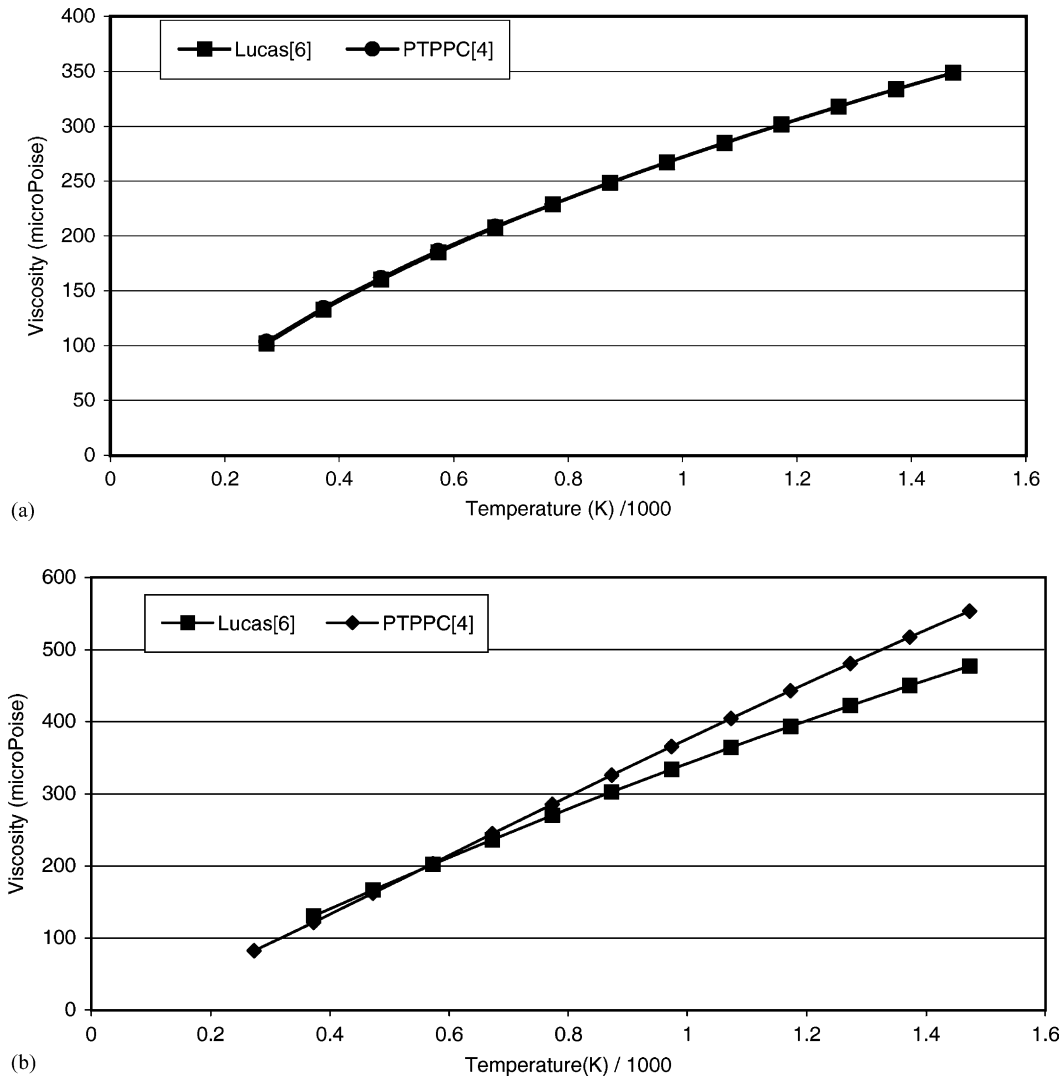

Fig. 1. Dynamic viscosity of CH_4 and H_2O as functions of temperature. Each graph shows the PTPPC experimental data and a representative estimation technique. (a) CH_4 (non-polar) and (b) H_2O (strongly polar).

sets available and estimation techniques are less reliable. PTPPC data has been favoured but two other data sets (which agree closely with PTPPC over the PTPPC range and extend to higher temperatures) were also used. These are the CO_2 data set of Vukalovich and Altunin [8] and the UK Steam Tables [9]. The temptation to generate hybrid data compilations was resisted as this could result in inappropriate weighting towards more commonly used, but not necessarily more accurate, primary data. Instead, extrapolation was preferred, in particular for PTPPC CH_4 data from 1373 to 1473 K, and UK Steam Table data from 1273 to 1473 K. Species for which there are no reliable alternative data sets (CO, N_2, C_2H_6 and C_3H_8) are, fortuitously, species for which the Chung et al. estimation method [6] gives values within the specified experimental uncertainty of PTPPC and hence this method was used for these species. Table 3 lists the polynomial coefficients obtained from a sixth-order least-squares curve fit to the extended PTPPC data set. As before, the error associated with the curve fitting procedure is less than 0.1% between 273 and 1473 K. The 'error' specified in Table 3 is that given by PTPPC as experimental uncertainty. Values of thermal conductivity at 1473 K are included for verification purposes.

Fig. 2 illustrates the problems associated with polar gases. Fig. 2a is for non-polar CO_2 and Fig. 2b is for H_2O which is strongly polar. The poor performance of the estimation methods for the polar species is again evident. A comparison with Fig. 1 for viscosity highlights the greater uncertainty in the values of thermal conductivity.

6. Viscosity and thermal conductivity of gas mixtures

6.1. Dynamic viscosity of mixtures

There are no openly available experimental data compilations for the viscosity of the multi-component gas mixtures found in SOFCs. Nevertheless, data is available for most of

Table 3
Thermal conductivity, coefficients valid in the range 273−1473 K

	c_0	c_1	c_2	c_3	c_4	c_5	c_6	Error (%)	$\lambda \times 10^2$ (1473 K)
Ar	−0.1331	10.404	−18.610	26.039	−20.573	8.5311	−1.4444	10	5.5872
C_2H_6	−1.0512	10.289	−8.4738	47.376	−56.213	27.575	−5.0288	3	22.349
C_3H_8	−0.6922	5.4368	4.7955	24.955	−37.361	19.772	−3.7519	10	20.377
CH_4	0.4796	1.8732	37.413	−47.440	38.251	−17.283	3.2774	3	26.500
H_2O	2.0103	−7.9139	35.922	−41.390	35.993	−18.974	4.1531	1	16.303
CO_2	2.8888	−27.018	129.65	−233.29	216.83	−101.12	18.698	10	9.3512
CO	−0.2815	13.999	−23.186	36.018	−30.818	13.379	−2.3224	5	9.1172
H_2	1.5040	62.892	−47.190	47.763	−31.939	11.972	−1.8954	5	57.705
N_2	−0.3216	14.810	−25.473	38.837	−32.133	13.493	−2.2741	5	9.4124
O_2	−0.1857	11.118	−7.3734	6.7130	−4.1797	1.4910	−0.2278	10	9.9832

λ (W/m K) $= 0.01\sum_{k=0}^{6} c_k \tau^k$, where $\tau = T$ (K)/1000.

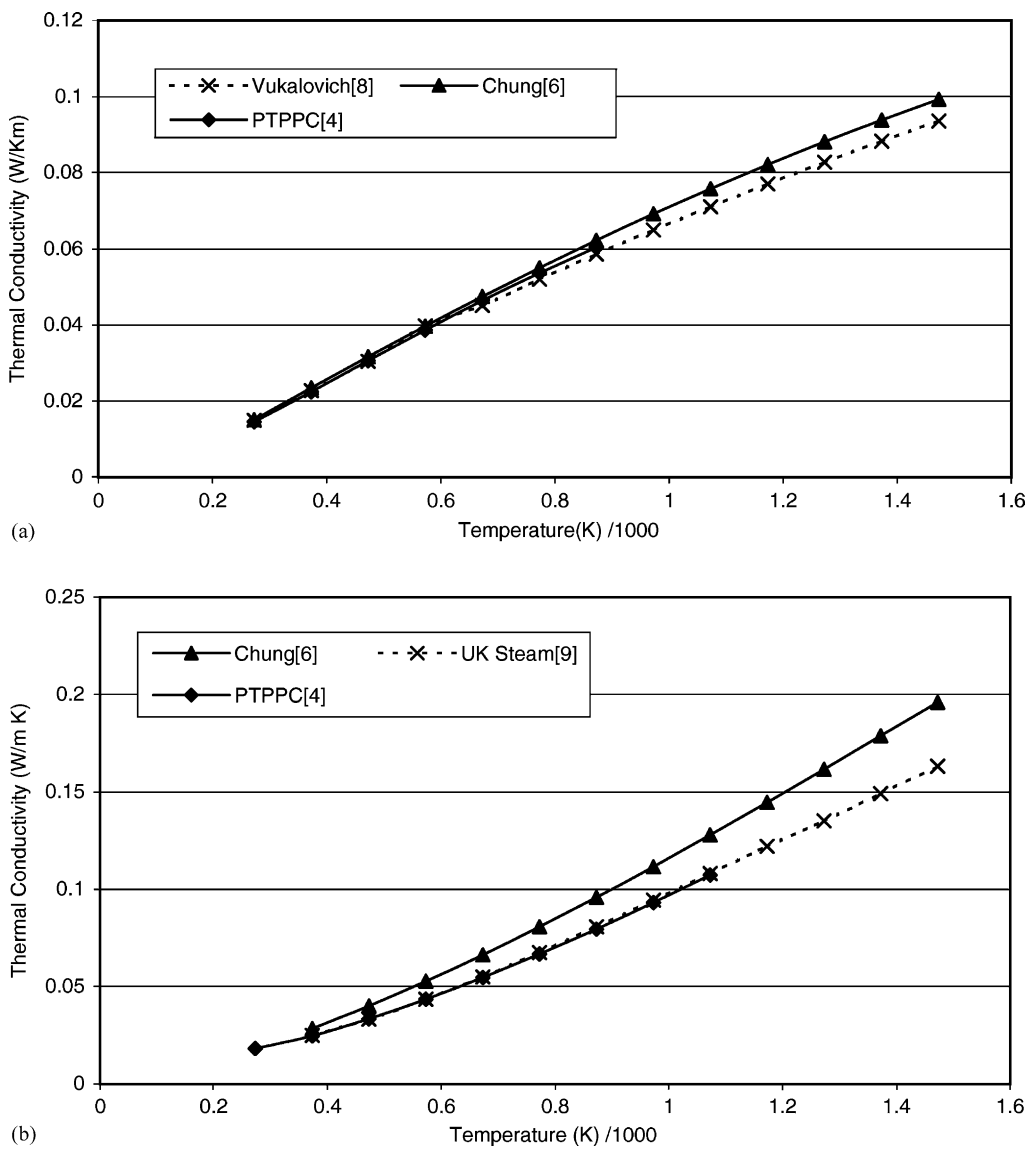

Fig. 2. Thermal conductivity of CO_2 and H_2O as functions of temperature. Each graph shows the extended PTPPC experimental data and a representative estimation technique. (a) CO_2 (non-polar), PTPPC data extended by Vukalovich and Altunin data. (b) H_2O (strongly polar), PTPPC data extended by UK Steam Table data.

Table 4
Deviation of estimated viscosity from experimental data for gas mixtures

Method	Mean deviation (%)	Maximum deviation (%)	Standard deviation (%)
Reichenberg	1.39	6.88	1.91
Herning and Zipperer	−2.15	−12.75	3.42
Wilke	2.18	15.05	2.87
Lucas	−3.86	−17.63	6.59
Chung et al.	−5.28	−23.76	7.13
Mole fraction averaging	−6.19	−30.13	8.53

the possible binary pairs and even for some multi-component mixtures [10,12]. Most of this data is for mixtures below 600 K, but this is not unduly problematic because investigation has shown that the deviation of estimation method values from the experimental data depends mainly on the mixture composition rather than the temperature (see below).

Six estimation methods for mixture viscosity were considered, all of which are described in Poling et al. [6]. These formulae were tested on 484 experimental data points, 282 of which were at a temperature above 400 K and 40 of which were at a temperature above 600 K. The mean, maximum and standard deviations from the experimental data are given in Table 4. The most accurate method was that of Reichenberg, which gave a mean deviation of 1.4%, with a maximum deviation of just 6.9%. This deviation is of the same order as the uncertainty in the experimental measurements. Unfortunately, Reichenberg's method is the most complex of the methods tested. If it is considered too cumbersome, the method of Herning and Zipperer is considerably simpler and still consistently accurate.

Fig. 3 shows the deviations of the values calculated by Reichenberg's method from the experimental measurements. All 484 data points are included and provide a graphic demonstration that the accuracy does not deteriorate with increasing temperature. This can be explained by reference to Fig. 4, which shows the variation of experimental viscosity data with composition for an O_2–H_2 mixture at various temperatures. If the mixture viscosity were a mole fraction average of the pure component values (like heat capacity), the curves would become straight lines connecting the pure component end points. Clearly this is

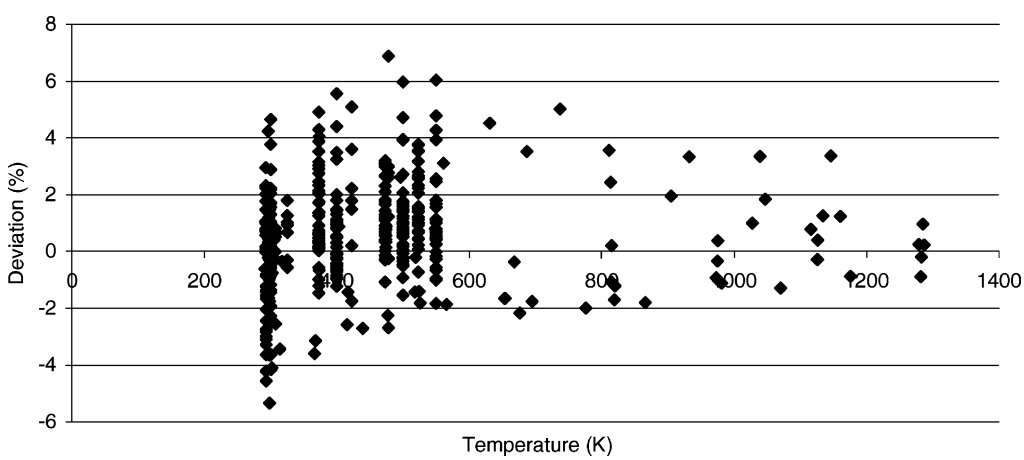

Fig. 3. Deviation of estimated viscosity (using Reichenberg's method) from experimental data (484 data points with a variety of mixture compositions).

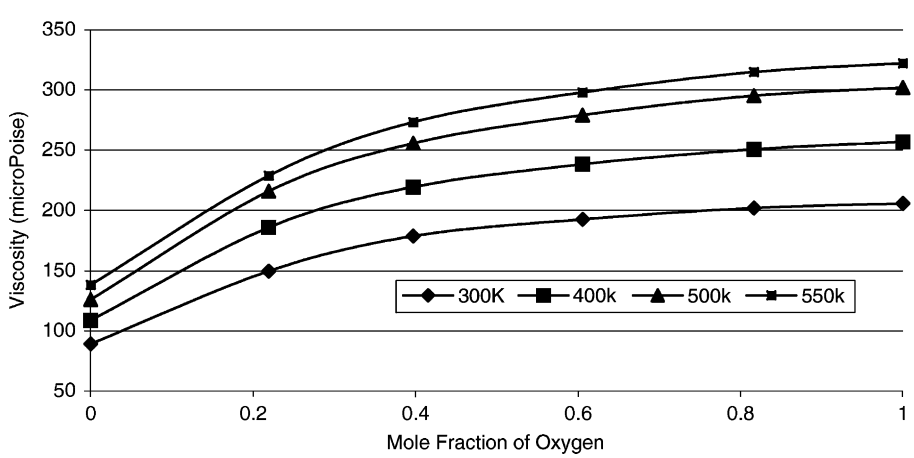

Fig. 4. Variation of experimental viscosity data with composition at different temperatures for an O_2–H_2 mixture. Note the similar shape of the four curves.

Table 5
Deviation of estimated thermal conductivity from experimental data for gas mixtures

Method	Mean deviation (%)	Maximum deviation (%)	Standard deviation (%)
W with M&S I	4.70	20.92	5.93
W with M&S II	5.33	25.38	6.47
Chung et al.	−12.51	−50.08	16.73
Mole fraction averaging	13.10	72.21	17.42

not the case and it is this variation from the mole fraction average which estimation techniques must capture. Now, considering the variation with temperature, it will be noted that the shape of the curves are very similar (being simply shifted to connect the appropriate pure component values). Hence, if an estimation technique can capture the shape at one temperature it can be expected to do so generally. This hypothesis is validated by the success of Reichenberg's method for that high temperature data which is available.

6.2. Thermal conductivity of mixtures

As with viscosity, there are no openly available experimental data compilations for the thermal conductivity of the multi-component gas mixtures found in SOFCs. However, data can be found for many of the possible binary pairs and for some multi-component mixtures [11,12].

Four estimation methods for the thermal conductivity of gas mixtures were considered, all of which are described in Poling et al. [6]. These formulae were tested on 431 experimental data points, 174 of which were at a temperature above 400 K and 83 of which were at a temperature above 600 K. The mean, maximum and standard deviations from the experimental data are given in Table 5. The most accurate method was found to be that of Wassiljewa with the Mason and Saxena modification which uses pure component viscosities to calculate the ratio of the pure component translational thermal conductivities (W with M&S I). The method gave a mean deviation of 4.70% with a maximum deviation of 20.92%. These values are significantly higher than those associated with Reichenberg's method for viscosity and result from the difficulty in modelling the contributions from the non-translational energy transfer. As might be expected, the maximum deviation was found to be for systems containing hydrogen, the effect of the highly directional hydrogen bond being poorly accounted for in the model.

Fig. 5 shows the deviations of the values calculated by the above method (W with M&S I) from the experimental measurements. All 431 data points are included and demonstrate (as for viscosity) that the accuracy of the estimation method does not, in general, deteriorate with increasing temperature. This can be explained in the same way as for viscosity (see Fig. 6 showing the variation of experimental thermal conductivity data with composition for a CO_2–H_2 mixture at various temperatures).

7. Binary diffusion coefficients

For the 10 gases considered in this study, there are 45 possible binary pairs each associated with a binary diffusion coefficient. Once determined, these coefficients can be used with the techniques of multi-component diffusion theory to calculate the component diffusive fluxes in the multi-component gas mixtures found in SOFCs. The problem, therefore, is how to represent the 45 binary diffusion coefficients as functions of temperature. One obvious approach (given that binary diffusion coefficients are independent of composition) is to provide curve fits to experimental measurements for each binary pair. This, however, is not feasible as the available data for most binary pairs is too sparse to allow accurate generation of the empirical curves. Indeed, a search of the literature [13–22] yielded a total data set of only 507 points of which 227 were for temperatures greater than 400 K and 83 for temperatures greater than 600 K. This represents an average of only 11 points per binary pair.

The alternative approach adopted here is to combine the data for all the binary pairs together and then determine

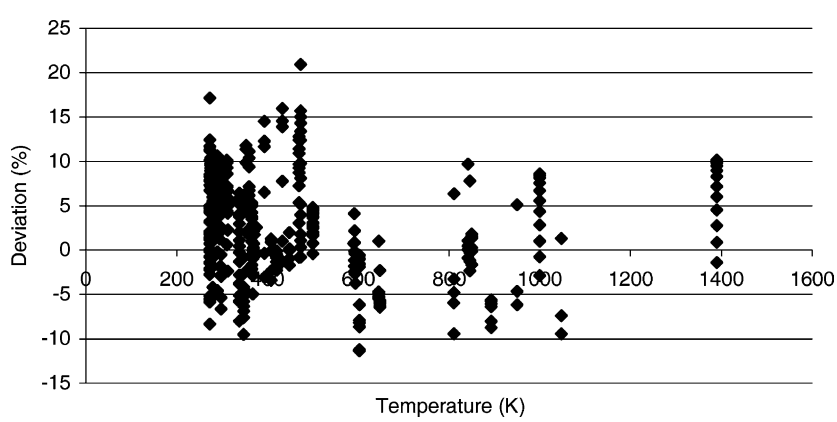

Fig. 5. Deviation of estimated thermal conductivity (using Wassiljewa with Mason and Saxena modification I) from experimental data (431 data points with a variety of mixture compositions).

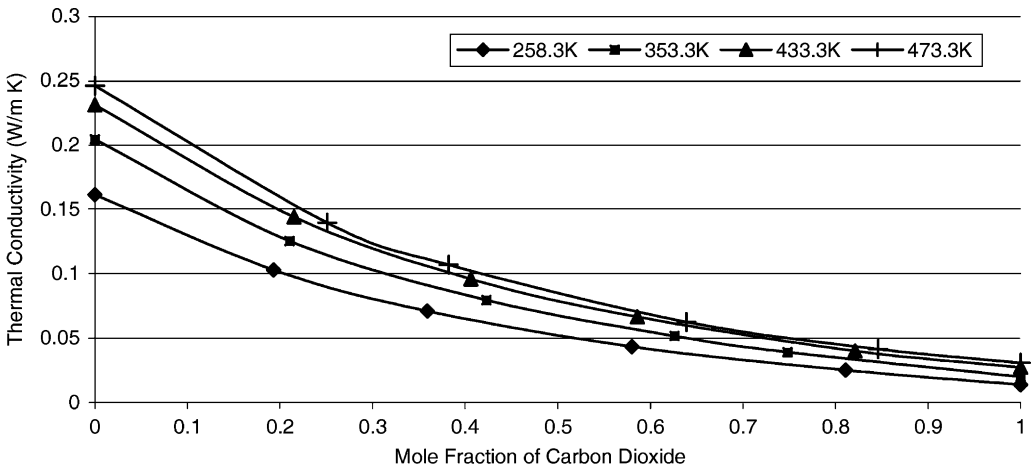

Fig. 6. Variation of experimental thermal conductivity data with composition at different temperatures for a CO_2–H_2 mixture. Note the similar shape of the four curves.

which of the available semi-theoretical estimation techniques best describes the overall data set. The four estimation methods considered are described by Poling et al. [6]. There are two kinetic theory based methods (one using the two-parameter Lennard–Jones potential, the other including a correction for polar molecules as suggested by Brokaw), and two correlations by Wilke and Lee and Fuller et al. which, although, still based on kinetic theory, involve more empiricism. The method of Fuller et al. is by far the simplest, retaining only the basic form of the kinetic theory diffusion coefficient equation.

As typical examples, Fig. 7 shows the variation with temperature of the diffusion coefficients of H_2–CO and H_2–H_2O mixtures (the latter being of particular importance for SOFC calculations). Included are four curves corresponding to the estimation methods described above together with the available experimental data. The somewhat disheartening conclusion is that the estimation methods seem to agree closely at low temperature (where data is available) but diverge significantly at high temperature (where there is no data). Closer investigation reveals, however, that the apparent agreement at low temperature is actually related to the scale of the ordinate.

To illustrate this further, Fig. 8 is a plot for O_2–H_2 mixtures where some high temperature experimental data is actually available. Plotting the percentage deviation of the estimated value from the experimental value, shows that the method of Fuller et al. performs better than the other methods at low temperature. Furthermore, the deviation of the method of Fuller et al. is essentially independent of temperature. It, therefore, appears that the accuracy of an estimation method at low temperature can give some indication of its accuracy at high temperature.

In the method of Fuller et al., the diffusion coefficient is proportional to temperature raised to the power 1.75 and this results in high temperature values for some species pairs being 10–20% higher than the predictions of other kinetic theory methods. Indeed, as noted by Fuller et al. [22], "the first limitation of kinetic theory is the 1.5 power temperature dependence; observed values usually lie in the range 1.6–1.8." It should be noted, however, that the lower temperature power found in the other kinetic theory methods is partially offset by a temperature dependent 'collision integral'. Full compensation is not obtained, however, unless a correction is made for 'molecular softening' at high temperatures. In the Lennard–Jones model, for example, the collision diameter, which is constant, should decrease with increasing temperature.

An overall assessment of all the estimation techniques applied to all possible binary pairs reveals that the method of Fuller et al. is the most consistent with the experimental data. Table 6 shows the performance of the various techniques averaged over all binary pairs. The method of Fuller et al. gives a mean error of −4.47%, a maximum error of 34.10% and a standard deviation of 7.73%. Fig. 9 shows the deviations of the values calculated by the method of Fuller et al. from the experimental measurements for all binary pair data points as a function of temperature. The fact that the deviation does not increase with temperature shows that the 1.75 temperature power dependence is a good approximation, at least in describing the experimental data currently available.

Table 6
Deviation of estimated diffusion coefficients from experimental data for binary gas mixtures (all species included)

Method	Mean deviation (%)	Maximum deviation (%)	Standard deviation (%)
Fuller et al.	4.47	34.10	7.73
Wilke and Lee	−13.12	−36.15	13.02
Lennard–Jones	−7.67	−34.47	6.34
Brokaw	−10.27	31.10	8.77

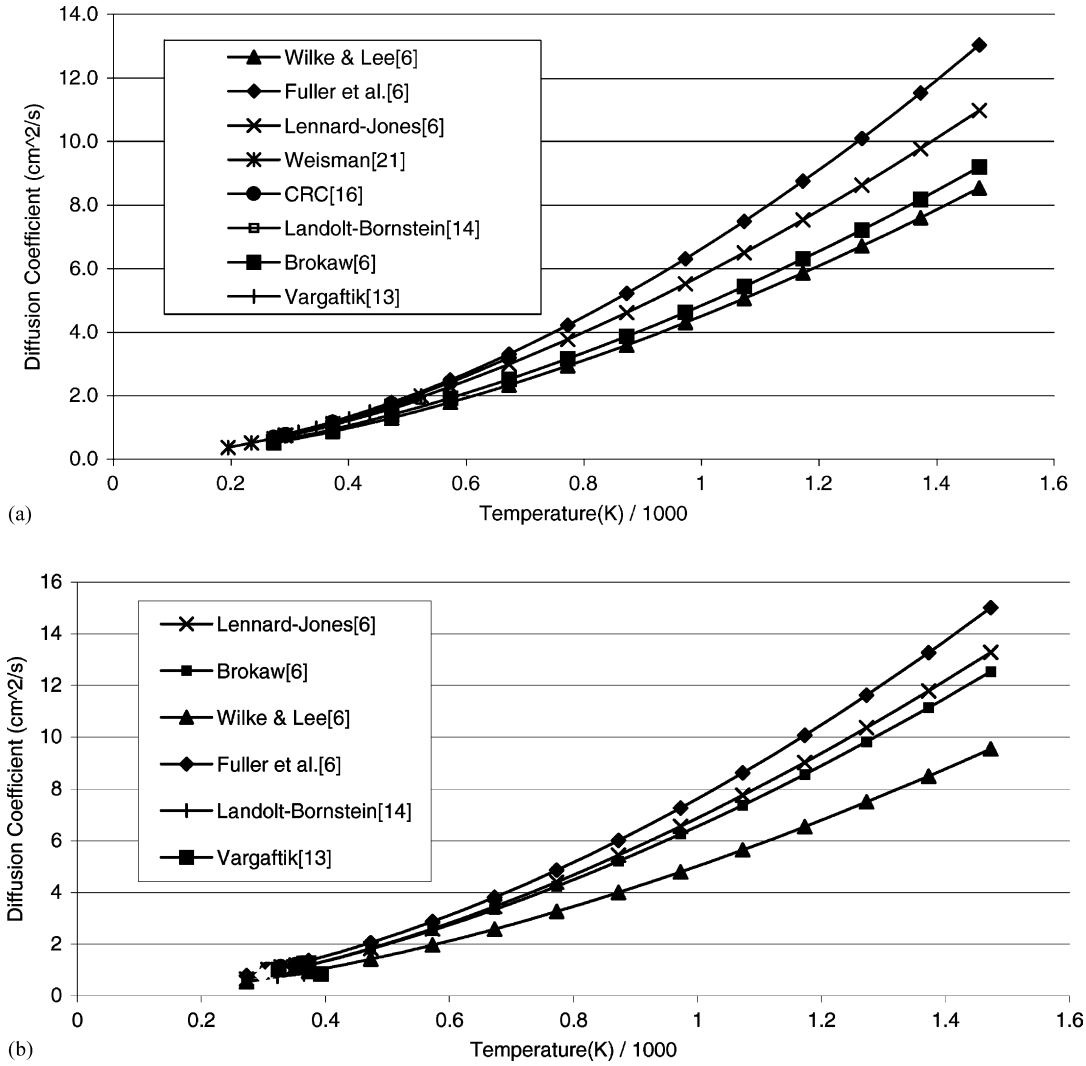

Fig. 7. Binary diffusion coefficients of H_2–CO and H_2–H_2O mixtures as functions of temperature. On each graph, the curves represent the four estimation methods and the remaining points show the experimental data which is all at low temperature. (a) H_2–CO and (b) H_2–H_2O.

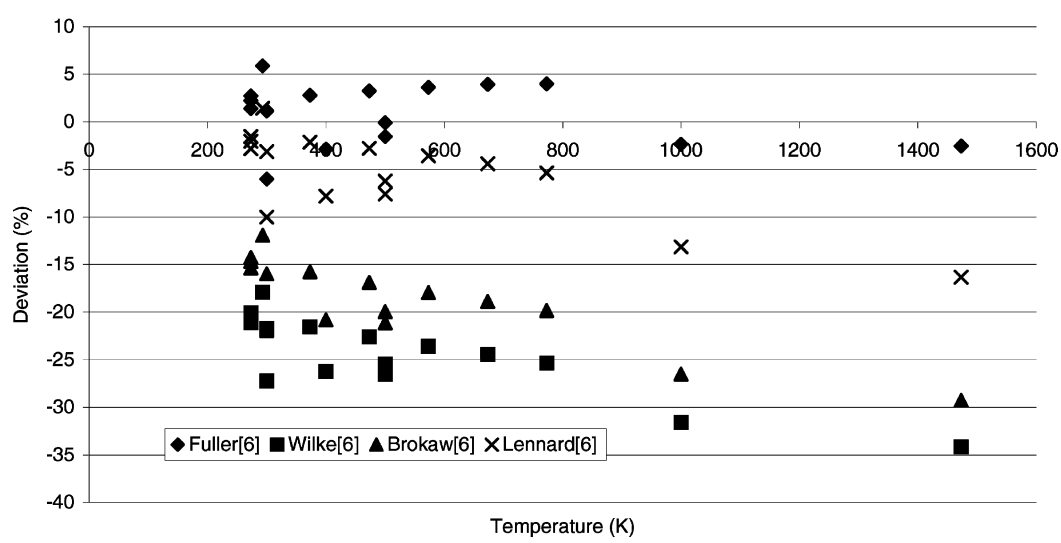

Fig. 8. Percentage deviation of estimated values of binary diffusion coefficient (four methods) from experimental data for O_2–H_2 mixtures as a function of temperature. The method of Fuller et al. is consistently accurate over the whole temperature range.

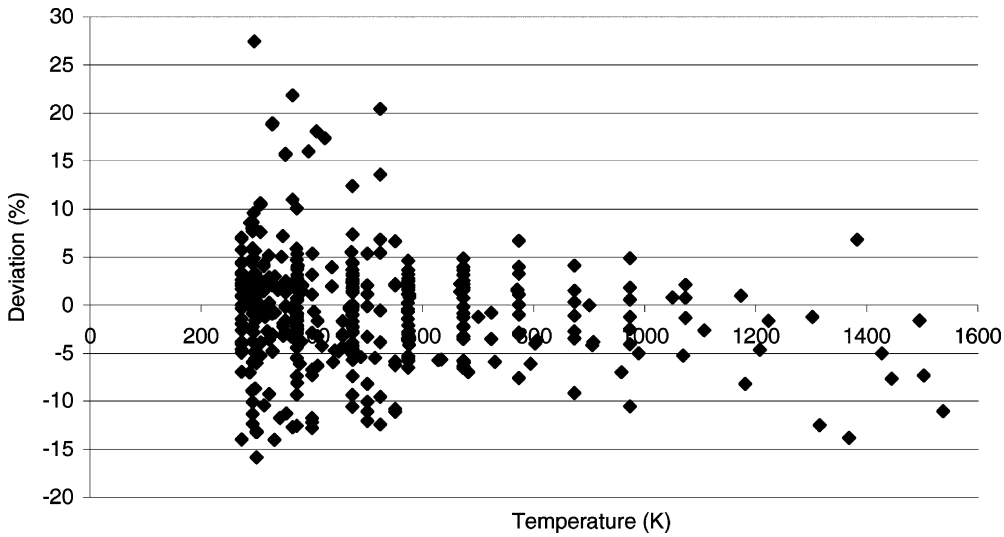

Fig. 9. Deviation of diffusion coefficients (estimated using the method of Fuller et al.) from experimental data as a function of temperature (all species included).

The few highly scattered points seen in Fig. 9 and the fact that, for the method of Fuller et al., the difference between the mean and maximum errors is three to four times larger than the standard deviation, suggests that the maximum error represents an anomaly. To investigate this in more detail, the data points have been divided according to binary pair and evaluated independently (using the method of Fuller et al.). This breakdown is presented in Table 7. There it can be seen that the maximum error of 34.10% occurs for the binary pair H_2O–CO_2 and that without this data set the maximum error would be reduced to 20.44%. What this breakdown does not show, however, is that already one experimental data set for this binary pair (CRC [16]) has been discarded due to its dubious temperature dependence (see Fig. 10) and, if it were included, the maximum deviation would rise to 45%. Why there is such variation in experimental data for this particular binary pair is unclear (although Fig. 10 shows that Fuller's method over-estimates the diffusion coefficient at ambient temperature resulting in poor performance even at low temperature). For this particular data set, the method of Wilke and Lee is rather more accurate (giving mean and maximum deviations of 4.26 and −7.5%, respectively for the reduced data set) and so could be used if desired. However, for this particular binary pair, the methods of Fuller et al. and Wilke and Lee have very similar temperature dependence which means that at the high temperatures of interest for SOFC applications the discrepancy which gives such large errors at ambient conditions becomes

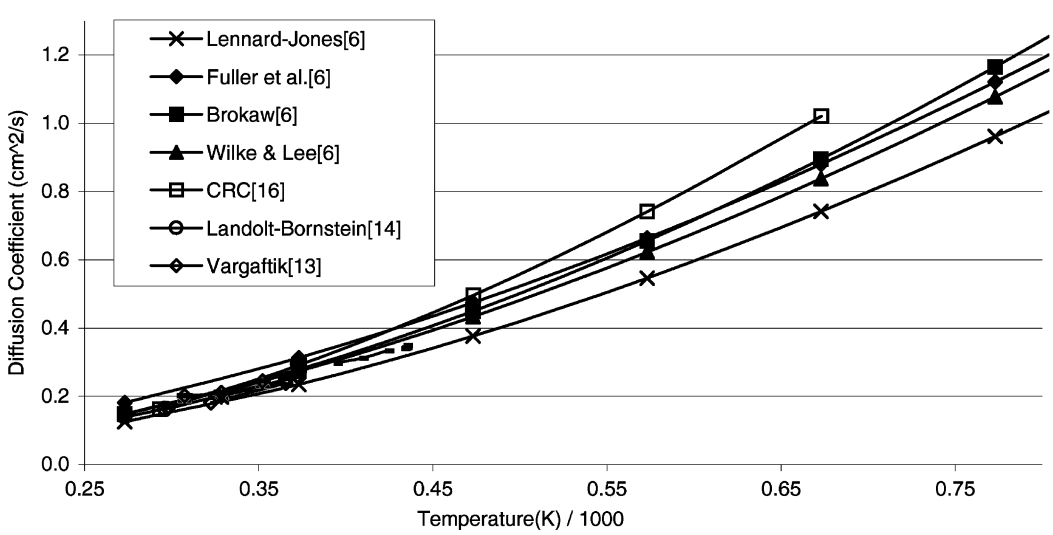

Fig. 10. Binary diffusion coefficient of H_2O–CO_2 as a function of temperature (273–800 K). The CRC data set shows anomalous behaviour and has not been included in the analysis.

Table 7
Deviation of estimated values for diffusion coefficients (using the method of Fuller et al.) from experimental values for each binary pair of gases

	N_2	O_2	H_2	H_2O	CO	CO_2	CH_4	Ar	C_2H_6
O_2	19 (3)[a]								
	1.69[b]								
	−7.62[c]								
	2.36[d]								
H_2	41 (8)	16 (4)							
	−3.36	2.90							
	−8.90	−6.03							
	4.23	3.81							
H_2O	13 (0)	22 (9)	17 (0)						
	5.71	−3.21	6.77						
	−13.93	−7.41	14.14						
	7.79	3.06	5.14						
CO	11 (1)	12 (4)	24 (1)						
	−6.07	−2.37	5.00						
	−14.02	−5.53	13.59						
	4.13	3.83	3.51						
CO_2	44 (11)	15 (4)	52 (12)	14 (0)	12 (0)				
	−4.71	−2.44	−3.46	20.91	−2.77				
	−13.84	4.39	12.54	34.1	7.94				
	4.81	3.58	5.34	7.72	4.42				
CH_4	8 (1)	10 (4)	19 (1)	11 (0)	6 (0)	3 (0)			
	1.92	−5.09	−5.20	3.65	0.75	2.22			
	−3.81	−6.99	−12.55	5.63	2.11	5.73			
	2.21	4.87	3.98	3.93	1.12	3.09			
Ar	11 (1)	19 (3)	38 (6)		7 (1)	24 (8)	4 (1)		
	2.51	2.70	−3.09		3.16	−6.16	2.78		
	7.07	−5.31	−6.97		4.90	−13.81	3.80		
	3.10	2.72	3.22		1.00	8.27	0.85		
C_2H_6	1 (0)		5 (0)	1 (0)			4 (0)		
	−0.85		3.06	3.28			9.89		
	−0.85		5.43	3.28			20.44		
	0		2.03	0			16.08		
C_3H_8			5 (0)	1 (0)		8 (0)	4 (0)		6 (0)
			3.43	−5.6		−5.88	−17.61		−5.37
			6.66	−5.6		−10.81	−19.90		−12.41
			2.59	0		9.09	1.90		6.56

[a] Total number of data points (number with T > 600 K).
[b] Mean deviation (%).
[c] Maximum deviation (%).
[d] Standard deviation (%).

insignificant. In the interests of consistency, therefore, it is recommended that the method of Fuller et al. be used, even for this binary pair.

8. Comparison with the international energy agency (IEA) SOFC handbook

It is of interest to compare the data assembled here with that presented in the IEA SOFC Handbook [23].

The cubic expressions supplied by the IEA for heat capacity yield values within 1% of those from the sextic expressions given in Table 1. In most cases, the IEA quadratic expressions for viscosity and thermal conductivity yield values within 5% of those from the sextic expressions given in Tables 2 and 3. There are, however, a few notable exceptions, particularly at the extremes of the temperature range, for example:

Viscosity	H_2O	273 K	Deviation	46%
Viscosity	CO	273 K	Deviation	17%
Thermal conductivity	H_2O	373 K	Deviation	12%
Thermal conductivity	CH_4	1473 K	Deviation	22%

These deviations are probably due either to the use of a less accurate estimation technique or to the use of a curve fit to data over a reduced temperature range. Thus, the IEA data

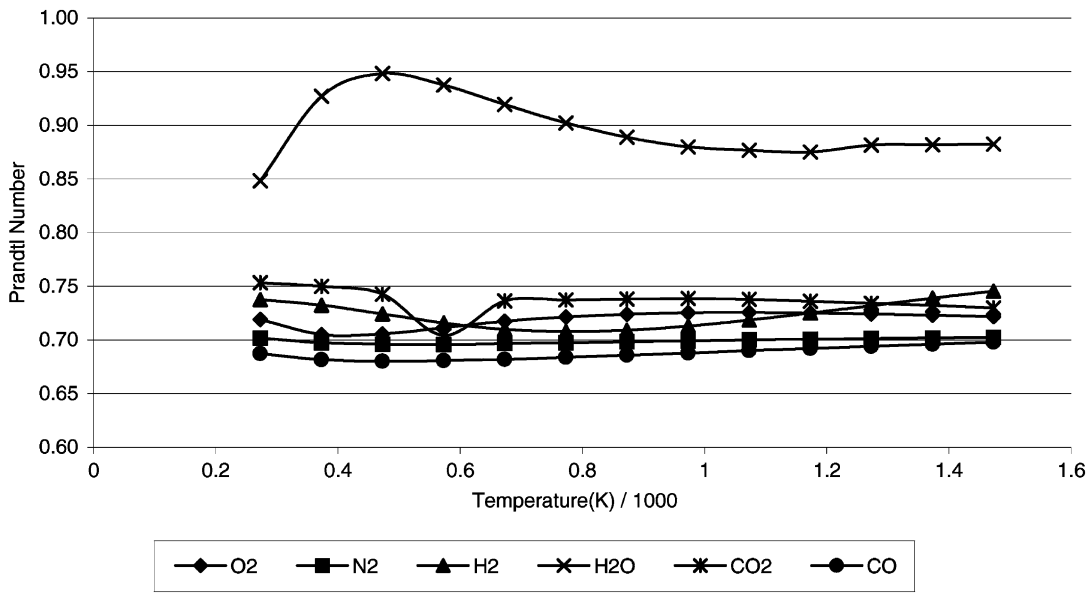

Fig. 11. Variation of Prandtl number with temperature for key SOFC gases.

for H_2O viscosity agree well with Lucas's method rather than with the PTPPC experimental data (see Fig. 1b).

The IEA Handbook gives only limited diffusion coefficient data (mainly from Perry [15]), all of which has been evaluated in the present study, and gives no data for the viscosity or thermal conductivity of gas mixtures.

9. Evaluation of dimensionless groups

The thermodynamic and transport properties can be combined to form several dimensionless groups, widely used in modelling. Of particular interest are the Prandtl and Schmidt numbers, from which the Lewis number can also be obtained. The Prandtl number,

$$Pr = \frac{C_p \mu}{\lambda}$$

is the ratio of viscous and thermal diffusivities while the Schmidt number,

$$Sc = \frac{\mu}{\rho D_{AB}}$$

is the ratio of viscous and mass diffusivities. It should be noted that both Pr and Sc vary with mixture composition.

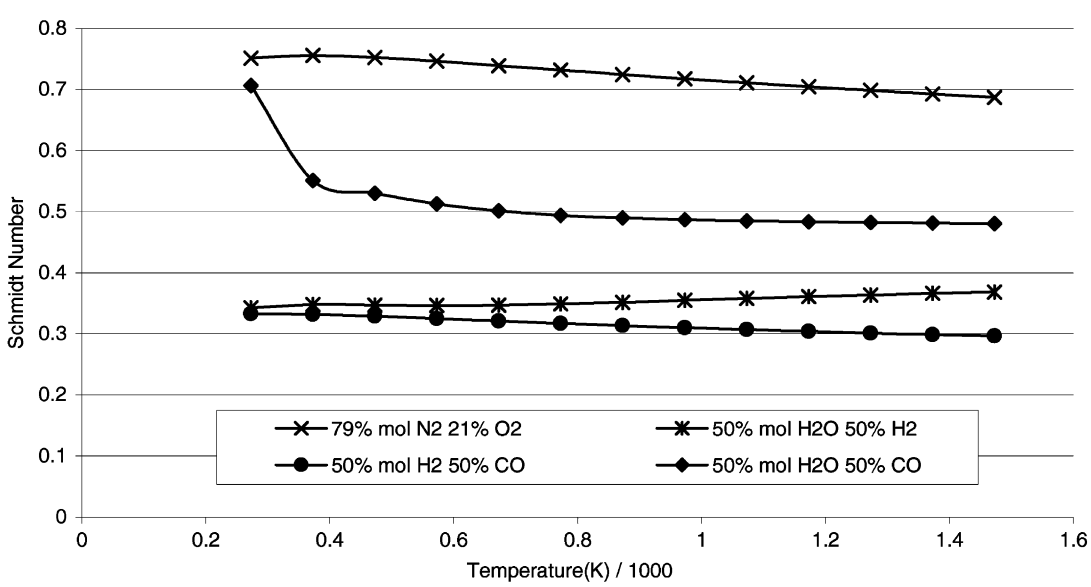

Fig. 12. Variation of Schmidt number with temperature for key SOFC gas mixtures.

Fig. 11 shows the variation of the Prandtl number with temperature for a selection of pure SOFC gases. It is very useful to see that Pr is largely independent of temperature (typically 5–10% variation) as predicted by simple kinetic theory. The largest discrepancy is in the case of H_2O (11%), which is not surprising given the polar nature of the molecules. Values of Prandtl number are in the range 0.68–0.75 for all gases except H_2O for which it is in the range 0.85–0.95.

Fig. 12 shows the variation of Schmidt number for air (molar 79% N_2 and 21% O_2), and for equimolar mixtures of H_2–H_2O, H_2–CO and H_2O–CO. The temperature dependence is stronger than for Prandtl number, being of the order 10–20% and up to 40% in the case of H_2O–CO. There is also significant variation in *Sc* between gas pairs, with magnitudes in the range 0.3–0.8.

10. Conclusions

Sixth-order, least-squares polynomial curve fits to experimental data for pure gases have been calculated for the following thermodynamic and transport properties:

1. Isobaric molar heat capacity (mean error 1% and maximum error 3%).
2. Dynamic viscosity (mean error 5% and maximum error 10%).
3. Thermal conductivity (mean error 6% and maximum error 10%).

For multi-component gas mixtures the following recommendations are made:

1. Isobaric molar heat capacity can be calculated by mole fraction averaging with errors of the same magnitude as the uncertainty in the pure component data.
2. Dynamic viscosity can be calculated by Reichenberg's method with an estimated mean error of 5% and maximum error of under 10%.
3. Thermal conductivity can be calculated using the Wassiljewa equation with the modification of Mason and Saxena (using pure component viscosities to calculate the ratio of thermal conductivities) with an estimated mean error of 6% and a maximum error of about 20%.

Experimental data for binary diffusion coefficients are very scarce, particularly at the high temperatures required. Fuller's method is recommended for all binary pairs with an estimated mean error of 5% but a maximum error of over 20%. This is the best recommendation that can be made with the available data. Further reliable experimental data, particularly for mixtures of CH_4, H_2O, CO_2, CO and H_2 would be of great benefit.

The single component data presented here is considered more accurate than that given in the 1992 IEA SOFC Handbook [23]. Discrepancies in the IEA data are typically of the order of 5%, but in several cases up to 25%.

The dimensionless Prandtl and Schmidt numbers can be taken to be independent of temperature with errors of 5–10 and 10–20%, respectively. The mean Prandtl number of SOFC gas flows can be expected to be between 0.7 and 0.9 depending primarily on H_2O content. The Schmidt number of SOFC gas mixtures is more sensitive to changes in all gas mole fractions and lies in the range 0.3–0.8.

11. Further work

This is an ongoing project. Contributions would be greatly appreciated and further results will be presented online as they emerge at http://www.FuelCellKnowledge.org/.

Acknowledgements

The work was carried out at the Hopkinson Laboratory, Cambridge University Engineering Department and B. Todd was supported by an EPSRC research studentship with a CASE award from Rolls-Royce plc, Derby. The authors are grateful to Dr. G. Agnew and Dr. C. Adderley of Rolls-Royce for their support and technical advice.

Appendix A. Recommended estimation methods and gas property data bank

A.1. Dynamic viscosity of multi-component gas mixtures

Reichenberg's expression for the dynamic viscosity of a mixture of *n* component gases is (see Poling et al. [6])

$$\eta_{\mathrm{m}} = \sum_{i=1}^{n} K_i \left(1 + 2\sum_{j=1}^{i=1} H_{ij} K_j + \sum_{j=1\neq i}^{n} \sum_{k=1\neq i}^{n} H_{ij} H_{ik} K_j K_k \right)$$

where

$$K_i = \frac{y_i \eta_i}{y_i + \eta_i \sum_{k=1\neq i}^{n} y_k H_{ik} [3 + (2M_k/M_i)]},$$

$$H_{ij} = \left[\frac{M_i M_j}{32(M_i + M_j)^3} \right]^{1/2} \times (C_i + C_j)^2 \frac{[1 + 0.36 T_{\mathrm{r}ij}(T_{\mathrm{r}ij} - 1)]^{1/6} F_{\mathrm{R}ij}}{T_{\mathrm{r}ij}^{1/2}}$$

where

$$C_i = \frac{M_i^{1/4}}{(\eta_i U_i)^{1/2}}, \qquad U_i = \frac{[1 + 0.36 T_{\mathrm{r}i}(T_{\mathrm{r}i} - 1)]^{1/6} F_{\mathrm{R}i}}{T_{\mathrm{r}i}^{1/2}},$$

$$T_{\mathrm{r}i} = \frac{T}{T_{\mathrm{c}i}}, \qquad F_{\mathrm{R}i} = \frac{T_{\mathrm{r}i}^{3.5} + (10\mu_{\mathrm{r}i})^7}{T_{\mathrm{r}i}^{3.5}[1 + (10\mu_{\mathrm{r}i})^7]},$$

$$\mu_{ri} = 52.46\frac{\mu_i^2 p_{ci}}{T_{ci}^2}, \qquad T_{rij} = \frac{T}{(T_{ci}T_{cj})^{1/2}},$$

$$F_{Rij} = \frac{T_{rij}^{3.5} + (10\mu_{rij})^7}{T_{rij}^{3.5}[1 + (10\mu_{rij})^7]}, \qquad \mu_{rij} = (\mu_{ri}\mu_{rj})^{1/2}$$

here η_m: dynamic viscosity of gas mixture (μP); η_i: dynamic viscosity of pure component i (μP); y_i: mole fraction of component i; M_i: molar mass of component i (kg/kmol); μ_i: dipole moment of component i (debye); T: temperature (K); T_{ci}: critical temperature of component i (K); p_{ci}: critical pressure of component i (bar).

A.2. Thermal conductivity of multi-component gas mixtures

Wassiljewa's expression for the thermal conductivity of a mixture of n component gases is (see Poling et al. [6]),

$$\lambda_m = \sum_{i=1}^{n} \frac{y_i\lambda_i}{\sum_{j=1}^{n} y_j A_{ij}}$$

where given by the Mason and Saxena modification,

$$A_{ij} = \frac{\varepsilon[1 + (\lambda_{tri}/\lambda_{trj})^{1/2}(M_i/M_j)^{1/4}]^2}{[8(1 + M_i/M_j)]^{1/2}}, \qquad \frac{\lambda_{tri}}{\lambda_{trj}} = \frac{\eta_i}{\eta_j}\frac{M_j}{M_i}$$

here λ_m: thermal conductivity of gas mixture (w/mK); λ_i: thermal conductivity of pure component I (w/mK); η_i: dynamic viscosity of pure component i (μP); y_i: mole fraction of component i, M_i: molar mass of component i (kg/kmol); ε: numerical constant near unity, taken as unity.

A.3. Binary diffusion coefficient

The Fuller et al. expression for the binary diffusion coefficient of a mixture of two gases A and B is (see Poling et al. [6]),

$$D_{AB} = \frac{0.00143T^{1.75}}{pM_{AB}^{1/2}[V_A^{1/3} + V_B^{1/3}]^2}$$

where

$$M_{AB} = 2[(1/M_A) + (1/M_B)]^{-1}$$

here D_{AB}: binary diffusion coefficient (cm^2/s); T: temperature (K); p: pressure (bar); M_A and M_B: molar mass (kg/kmol); V_A and V_B: special Fuller et al. diffusion volume.

A.4. Gas property data bank [6,24,25]

See Tables 8 and 9.

Table 8
Gas property data used in the calculation of the viscosity and thermal conductivity of multi-component gas mixtures and binary diffusion coefficients

	Molar mass (kg/kmol)	Critical temperature (K)	Critical pressure (bar)	Dipole moment (debye)	Fuller et al. diffusion volume
Ar	39.948	150.86	48.98	0	16.2
C_2H_6	30.07	305.32	48.72	0	45.66
C_3H_8	44.097	369.83	42.48	0	66.18
CH_4	16.043	190.56	45.99	0	25.14
H_2O	18.015	647.14	220.64	1.8	13.1
CO_2	44.01	304.12	73.74	0	26.7
CO	28.01	132.85	34.94	0.1	18.0
H_2	2.016	33.25	12.97	0	6.12
N_2	28.014	126.2	33.98	0	18.5
O_2	31.999	154.58	50.43	0	16.3

Table 9
Additional data required for pure gas property estimation techniques and alternative mixture and diffusion coefficient estimation techniques (for use in conjunction with [5] or [6])

	T_b (K)	V_c (cm^3/mol)	Z_c	ω	σ (Å)	η (K)	V_b (cm^3/mol)
Ar	39.948	150.86	0.291	−0.002	3.542	93.3	29.1
C_2H_6	30.07	305.32	0.279	0.099	4.443	215.7	46.15
C_3H_8	44.097	369.83	0.276	0.152	5.118	237.1	74.87
CH_4	16.043	190.56	0.286	0.011	3.758	148.6	35.54
H_2O	18.015	647.14	0.229	0.344	2.641	809.1	18.07
CO_2	44.01	304.12	0.274	0.225	3.941	195.2	28.176
CO	28.01	132.85	0.292	0.045	3.69	91.7	34.88
H_2	20.38	65	0.305	−0.216	2.827	59.7	28.475
N_2	77.35	90.1	0.289	0.037	3.798	71.4	34.84
O_2	90.17	73.37	0.288	0.025	3.467	106.7	27.85

References

[1] J.M. King, Applying fuel cell experience to sustainable power products, J. Power Sources 86 (2000) 16–22.

[2] E. Achenbach, Response of a solid oxide fuel cell to load change, J. Power Sources 57 (1995) 105–109.

[3] S. Chapman, T.G. Cowling, The Mathematical Theory of Non-Uniform Gases, 3rd Edition, Cambridge University Press, 1975.

[4] T.E. Daubert, R.P. Danner, Physical and Thermodynamic Properties of Pure Chemicals: Data Compilation, Taylor & Francis, Washington, DC, 1987.

[5] R.C. Reid, J.M. Prausnitz, B.E. Poling, The Properties of Liquids & Gases, 4th Edition, McGraw-Hill, New York, 1986.

[6] B.E. Poling, J.M. Prausnitz, J.P. O'Connell, The Properties of Liquids & Gases, 5th Edition, McGraw-Hill, New York, 2000.

[7] M.W. Chase Jr., C.A. Davies, J.R. Downey Jr., D.J. Frurip, R.A. McDonald, A.N. Syverud, JANAF Thermochemical Tables, 3rd Edition, American Institute of Physics, New York, 1986.

[8] M.P Vukalovich, V.V. Altunin, Thermophysical Properties of Carbon Dioxide, Collets, 1968.

[9] UK Steam Tables in S.I. Units 1970, Edward Arnold, London, 1970.

[10] Y.S. Touloukian (Ed.), Thermophysical Properties of Matter. The TPRC Data Series—Viscosity, Vol. 11, TPRC, New York, 1975.

[11] Y.S. Touloukian (Ed.), Thermophysical Properties of Matter. The TPRC Data Series—Thermal Conductivity, Vol. 3, TPRC, New York, 1970.

[12] K. Stephan, T. Heckenberger, Thermal Conductivity and Viscosity Data of Fluid Mixtures, DECHMA, Vol. X, Part 1, 1988.

[13] N.B. Vargaftik, Handbook of Physical Properties of Liquids and Gases: Pure Substances and Mixtures, Begell House, New York, 1996.

[14] Landolt-Bornstein, Numerical Data and Functional Relationships in Science and Technology, 6th Edition, Band II, Teil 5a, Springer, Berlin, 1950–1980.

[15] R.H. Perry, Perry's Chemical Engineering Handbook, 7th Edition, McGraw-Hill, New York, 1997.

[16] D.R. Lide (Ed.), CRC Handbook of Chemistry and Physics, 81st Edition, CRC Press, Boca Raton, 2000–2001.

[17] M. Schneider, K. Schafer, Gasdiffusionsmessungen zwischen 273 und 1300 K, Berichte der Bunsengesellschaft 73 (1969) 702–706.

[18] J.M. Hellemans, J. Kestin, S.T. Ro, The viscosity of oxygen and some of it's mixtures with other gases, Physica 65 (1973) 362–375.

[19] S. Gotoh, M. Manner, J.P. Sorenson, W.E. Stewart, Binary diffusion coefficients of low-density gases. 1. Measurements by modified Loschmidt method, J. Chem. Eng. Data 19 (1974) 169–171.

[20] C. R Mueller, Mass spectrometric measurement of diffusion coefficients, J. Chem. Phys. 40 (1964) 651–654.

[21] S. Weisman, E.A. Mason, Determination of gaseous-diffusion coefficients from viscosity measurements, J. Chem. Phys. 37 (1962) 1289–1299.

[22] E.N. Fuller, P.D. Schettler, J.C. Giddings, A new method for prediction of binary gas-phase diffusion coefficients, Ind. Eng. Chem. 58 (1966) 19–27.

[23] Facts & Figures, International Energy Association SOFC Task Report, Berne, April 1992.

[24] K. Raznjevic, Handbook of Thermodynamic Tables and Charts, Hemisphere, Washington, DC, 1976.

[25] IUPAC, Carbon Dioxide, Pergamon Press, Oxford, 1976.